TABLE I
COMPARISON OF MEASURED BIREFRINGENCE WITH SOME OTHER AVAILABLE VALUES

Measurement Frequency	1 kHz	95 GHz	245 GHz	245 GHz	600 GHz	890 GHz
Δn	0.047±.002*	0.047±.002*	0.0466±.0015	0.047±.001	0.0468±.003*	0.048±.001
reference	7	8	this work	this work	9	10
sample thickness	1.5 mm	4 mm	3.564 mm	6.000 mm	1.0497 mm, 4.7873 mm	0.228 mm to 25.71 mm

* Uncertainties have been conservatively deduced from information available in the references.

studied. The thickness measurement accuracy and actual thickness nonuniformities result in a thickness uncertainty of ± 0.01 mm. This is relatively crude when compared to sample thickness accuracies of some of the other references cited in Table I relating to the birefringence of crystalline quartz. However, our birefringence accuracy is still similar to theirs, since a sample thickness error in our experiments proportionately affects the *difference* between the ordinary and extraordinary indices, rather than the individual indices whose difference is usually subsequently taken. The quoted thickness uncertainty is actually somewhat conservative since the *average* thickness is more accurately known, and the average thickness determines the location of the signal minimum. The results are presented in Table I along with some other birefringence values from the work of others at neighboring frequencies. Our quoted results are actually each the average of several repetitions of the measurement. The other references were identified in an extensive survey of the NMMW materials spectroscopy literature [11]. Our 245-GHz results compare favorably with the other values. Our quoted uncertainty is based on the combined effects of the reproducibility of the micrometer settings and our estimate of possible systematic errors. Substantially greater accuracy can be achieved using this technique, if needed, by more elaborate attention to the procedure, sample preparation, and thickness measurement, and the use of thicker samples and lower leakage gratings.

ACKNOWLEDGMENT

The author wishes to express his appreciation for the timely loan of desirable crystal quartz samples by C. Tschiegg and A. Henins of the National Bureau of Standards, Gaithersburg, MD.

REFERENCES

[1] G. J. Simonis, F. Weiser, G. L. Wood, and J. M. Bowersett, "Fabrication, characterization, and applications of wire gratings for near-millimeter wave purposes," Harry Diamond Laboratories Tech. Rep., in preparation.
[2] A. Sentz, M. Pyee, C. Gastaud, J. Auvroy, and J. P. Letur, "Construction of parallel grids acting as semitransparent flat mirrors in the far infrared," *Rev. Sci. Instr.*, vol. 49, pp. 926–927, July 1978.
[3] D. H. Martin and E. Puplett, "Polarized interferometric spectrometry for the millimetre and submillimetre spectrum," *Infrared Phys.*, vol. 10, pp. 105–109, 1969.
[4] G. J. Simonis and R. D. Felock, "Near-millimeter wave polarizing duplexer/isolator," *Int. J. Inf. Millimeter Waves*, vol. 4, Mar. 1983.
[5] G. J. Simonis and R. D. Felock, "Index of refraction determination in the near-millimeter wavelength range using a mesh Fabry-Perot resonant cavity," *Appl. Opt.*, vol. 22, pp. 194–197, Jan. 1983.
[6] Y. Yamada, A. Mitsuishi, and H. Yoshinaga, "Transmission filters in the far-infrared region," *J. Opt. Soc. Am.*, vol. 52, pp. 17–19, Jan. 1962.
[7] J. Fontanella, C. Andeen, and D. Schuele, "Low-frequency dielectric constants of α-quartz, sapphire, MgF_2, and MgO," *J. Appl. Phys.*, vol. 45, pp. 2852–2854, July 1974.
[8] R. G. Jones, "The measurement of dielectric anisotropy using a microwave open resonator," *J. Phys. D: Appl. Phys.*, vol. 9, pp. 819–827, 1976.
[9] E. E. Russell and E. E. Bell, "Measurement of the optical constants of crystal quartz in the far infrared with the asymmetric Fourier-transform method," *J. Opt. Soc. Am.*, vol. 57, no. 3, pp. 341–348, Mar. 1967.
[10] D. Charlemagne and A. Hadni, "Sur la biréfringence et le pouvoir rotatoire du quartz dans l'infrarouge lointain à la température de l'azote liquide et a température ordinaire," *Optica Acta*, vol. 16, no. 1, pp. 53–60, 1969.
[11] G. J. Simonis, "Index to the literature dealing with the near-millimeter-wave properties of materials," *Int. J. Infrared Millimeter Waves*, vol. 3, pp. 439–469, July 1982.

Large Signal Design of GaAs FET Oscillators Using Input Dielectric Resonators

ABELARDO PODCAMENI, MEMBER, IEEE, AND LUIS AFONSO BERMUDEZ, MEMBER, IEEE

***Abstract*—A dielectric resonator may be placed at the input of an active two-port device (FET or microwave transistor) yielding a stable frequency source. For this input configuration, a large signal design is presented. The method is simple, and power output prevision is also reached. The practical results obtained with an *X*-band medium-power oscillator are presented.**

I. INTRODUCTION

Frequency-stable microwave sources are utilized in telecommunications and strategic applications. The GaAs FET is an efficient device for power generation from about 4 GHz upwards [1]. The frequency stabilization with a dielectric resonator [2] may contribute to obtain compact, lightweight, and economical oscillators.

In a previous work, Abe *et al.* [3] have presented a particular configuration using the dielectric resonator as a band-stop filter [4]. More recently, Mori *et al.* [5] used the dielectrical resonator as a frequency selective feedback device yielding a basic oscillator covering the 9–14-GHz band. However, neither of these two design methods is straightforward. Experimental adjustments were necessary, and if an output power prevision is desired, troublesome large signal analysis [6]–[9] must be carried out.

On the other hand, the configuration which uses the dielectric resonator placed at the FET input is also possible [10], [11]. However, a simple procedure taking into account large signal effects is not presently available. Hence, in this short paper, this oscillator configuration together with large signal analysis will be focused on. The resonator operates as a reflection-mode resonant cavity. Large signal measurements will yield the existing oscillatory conditions at the FET input. The dielectric resonator is then easily positioned. Similarly, an accurate output prevision may also be performed. This approach has been successfully used for fixed and narrow-band oscillators and consists, basically, of two steps: characterizing the resonator, and obtaining simplified large signal data from the active device.

II. DIELECTRIC RESONATOR CHARACTERIZATION

When a dielectric resonator is placed beside a microstrip line, magnetic field coupling will exist. Usually, for this type of application, a cylindrical resonator is preferred. In this case, the

Manuscript received July 22, 1982; revised November 29, 1982. This work was supported by Telecomunicações Brasileiras S/A under contracts 017/79 and 88/80 PUC-TELEBRÁS.

A. Podcameni is with the Universidade Católica do Rio de Janeiro, Rua Marques de São Vincente 209, Rio de Janeiro 22453, RJ Brasil.
L. Bermudez is with the Departmento de Engenharia Elétrico, Universidade de Brasilia, Brasilia, 70910, DF Brasil

0018-9480/83/0400-0358$01.00 ©1983 IEEE

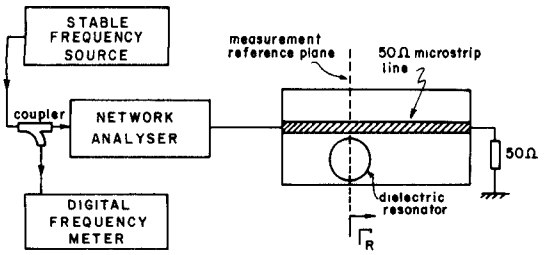

Fig. 1. Set up for dielectric resonator characterization.

relevant resonant mode is the $TE_{01\delta}$ [12], which may be easily tuned, typically over a band of about 10 percent. The resonator is then tuned to the desired frequency and the setup of Fig. 1 is used. Using a network analyzer, a stable frequency source, and a digital frequency meter, the reflection coefficient Γ_R at the resonant frequency ω_0 is obtained. This reflection coefficient will be real and positive.

Another important measurement which may be performed is for the unloaded quality factor Q_0, as seen from the microstrip line. For doing so, first, the Γ_R locus with respect to the frequency is obtained on the network analyzer. Next, the interceptions of Γ_R locus with the $R-1=\pm jX$ arcs are determined on the Smith chart. The value of Q_0 is then easily computed, as described elsewhere [13]. As the resonator works in the reflection mode, the modulus of Γ_R should be, ideally, unitary. However, when the resonator is placed far from the microstrip line, a very small value of $|\Gamma_R|$ will be observed: the resonator is not coupled to the line and the Q_0 measured will be also zero. As the resonator is moved towards the microstrip, both Γ_R and Q_0 will increase. However, if the resonator gets too close to the line, or goes over the line, a substantial drop of Q_0 will be observed. So, a fair tradeoff is usually obtained with $|\Gamma_R| \cong 0.9$. It is worthwhile to note that while performing these measurements, the losses of the environment are computed together with those of the resonator itself. Hence, some relevant practical situations (such as polishing and/or silver plating the interior of the metallic enclosure, proximity of the metallic walls, substrate materials and substrate heights) may be evaluated with respect to the quality factor. Usually, when all these parameters are well chosen, the maximum value of Q_0 obtained will be quite close to the isolated quality factor of the resonator Q_{00}-value, which takes into account only the losses of the resonator itself.

III. Active Subassembly Characterization

An FET may be used to obtain an active subassembly suitable for oscillating purposes. Some means must be provided in a way so that the small signal input reflection coefficient S_{11} would exceed the unity. This is easily accomplished, for instance, by using serial and/or shunt feedback [14] and/or output circuitry [15].

In the final circuit, the dielectric resonator will be put at an electrical distance θ from the input reference plane of the subassembly. In this situation, the reflection coefficient of the resonator, seen from the reference plane of the subassembly, is expressed as follows:

$$\Gamma = \Gamma_R e^{-2j\theta} = |\Gamma_R| e^{-2j\theta}.$$

If an oscillatory condition takes place, then the following relation will hold at the steady-state:

$$1 = S'_{11} \cdot \Gamma = S'_{11} \cdot |\Gamma_R| \cdot e^{-2j\theta} \tag{1}$$

where S'_{11} stands for the values of S_{11} under stable oscillatory conditions. As Γ_R is independent of the oscillation level, S_{11} should obviously decrease in magnitude to fulfill (1). It is also clear from (1) that in the steady-state $|S'_{11}| = 1/|\Gamma_R|$. Hence, for the characterization of the active device, it is sufficient to measure the input reflection coefficient with a progressively increasing signal level, until the value of $1/|\Gamma_R|$ is reached. In this situation, not only the argument of S'_{11}, but also the active device output power P_{out}, are noted.

IV. Oscillator Design

By using the previously obtained values of $|\Gamma_R|$, $|S'_{11}|$, and $\arg S'_{11}$, the design procedure is easily accomplished. From (1), it follows that

$$\theta = \frac{1}{2} \arg S'_{11} + n\pi \tag{2}$$

with $n = 0, 1, 2, \cdots,$.

Hence, the physical distance at which the resonator must be placed, with respect to the active device reference plane, is

$$d = (\theta/2\pi)\lambda_m \tag{3}$$

where λ_m is the wavelength in the microstrip at ω_0. Usually, in (3), the value of θ is used with $n = 0$ yielding the minimum value of d. In certain practical cases, however, d may result smaller than the physical radius of the resonator. Another value of n is then selected. In any case, since the resonator is properly positioned, as given by (3), the output power furnished by the oscillator is expected to be P_{out}.

It must be pointed out that this approach is transparent to any existing FET output circuitry. Consequently, this structure may be designed aiming at power efficiency or low noise [16], and may be considered as incorporated in the subassembly characterization.

A word of caution must be added. It is advisable to characterize the dielectric resonator and the active device in a fairly broad band around ω_0, to avoid oscillatory conditions with non-$TE_{01\delta}$ modes.

V. Practical Results

A 30-mW X-band oscillator at 8570 MHz will illustrate this method. The application is a local oscillator for a Brasilian terrestrial digital radio relay link. The dielectric resonator used is a Thomson-CSF with $\epsilon_r \cong 39.5$, having a 6-mm diameter and 4-mm height. The characterization of this resonator was performed using an environment as close as possible to the final one, over a Rogers 6010 substrate with $\epsilon_r = 10.5$ and $H = 0.635$ mm. By varying the distance between the edges of the disk and the line, the result shown in Fig. 2 is obtained. The value of Q_0 initially increases as the disk gets closer to the line. It has a maximum, but for extremely tight-coupling conditions it falls drastically. The coupling condition chosen is the one which will render a maximum Q_0, about 4300, with a reflection coefficient $\Gamma_R \cong 0.9$. In this situation, the $TE_{01\delta}$ mode was the only one observed in the 8- to 9-GHz band.

The next step is to prepare an active subassembly. The medium-power Dexcel 3501A-CR-RES GaAs FET was used. Shunt feedback was provided at the chip level, and an output circuit was added. This last circuit is a dual purpose one. It further increases the S_{11} modulus and approaches the oscillator towards minimum noise conditions. The subassembly was measured in a band from 8 to 9 GHz, for several input signal levels, and the results are presented in Fig. 3. For small signal conditions $|S_{11}|$ has a pronounced peak, exceeding the unity in the vicinity of 8570 MHz, the desired frequency, but it rolls off outside this band. These are desirable features for assuring that the oscillations will build up at the desired band. As the input

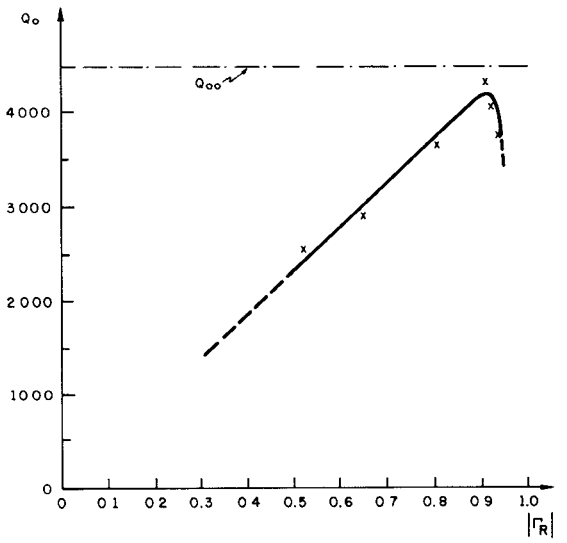

Fig. 2. Variation of the quality factor, as seen from the microstrip, for several coupling conditions.

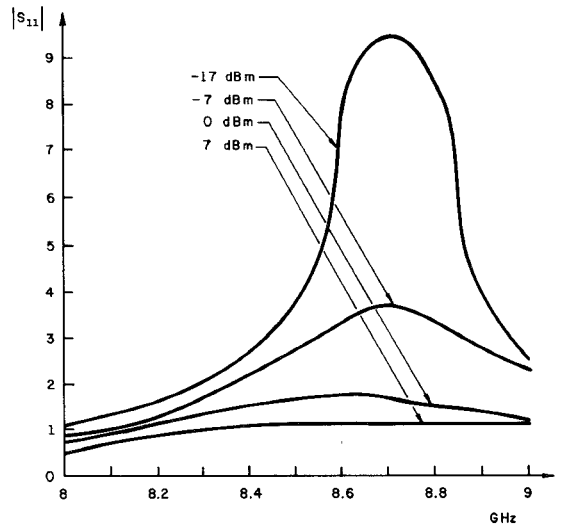

Fig. 3. Variation of the FET input reflection coefficient for several input power levels.

level is increased, saturation takes place. A more detailed aspect is given in Fig. 4. Here, the frequency is settled to 8570 MHz and the input power is progressively increased. The locus of $1/S_{11}$ is plotted. The phase of S_{11} varies with the amplitude, showing the importance of picking up the figure which corresponds to the exact operational condition. This one occurs when $1/|S_{11}| = |\Gamma_R| = 0.9$. In this saturation, $\arg S'_{11} = 173°$ is observed, and the output power furnished by the active subassembly was $P_{out} = 15.3$ dBm. It is worthwhile to note that around that point, the $1/S_{11}$ locus intercepts the Γ_R locus in an approximately orthogonal way. If this crossing were perfectly orthogonal, then a basic condition for minimum noise would be fulfilled [17]. In a Kurokawa's sense this would mean that the load and device line are perpendicular at the operation point.

By using the numerical value of $\arg S'_{11}$, and expressions (2) and (3), the distance d is obtained, with $n = 1$, yielding $d = 9.6$ mm. The oscillator was then mounted, and a schematic layout is presented in Fig. 5.

The initial practical tests furnished stable oscillations with an output power level of 15.5 dBm, very close to the predicted value.

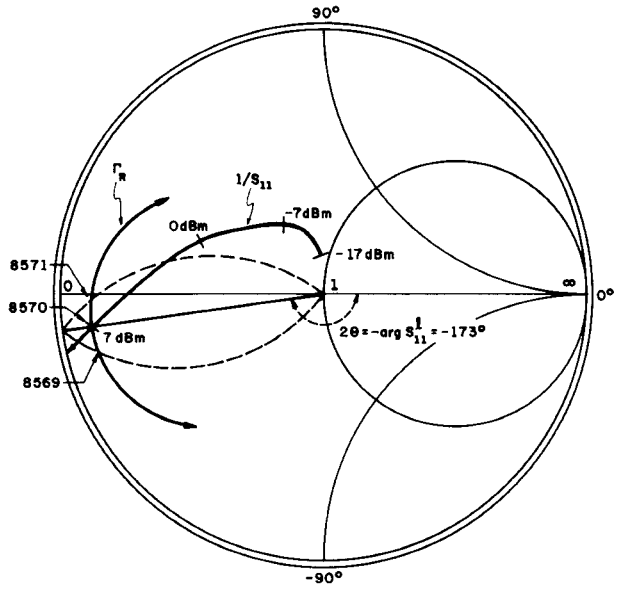

Fig. 4. Variation of S_{11} with respect to the input signal level at 8570 MHz. The figure shows the interception of $1/S_{11}$ locus with Γ_R locus. Power levels refer to FET input, frequencies are in megahertz.

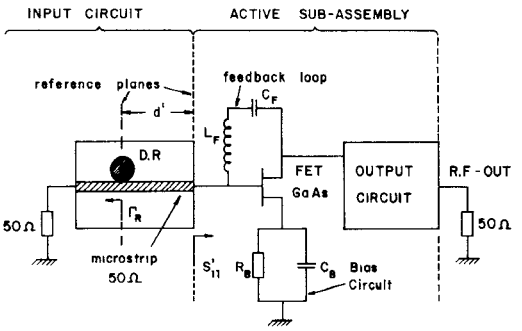

Fig. 5. Schematic layout of the FET Oscillator using an input dielectric resonator.

The frequency was also very close to the desired one. It was measured at 8584 MHz. By adjusting a tuning screw over the resonator the frequency was easily brought to the desired value with negligible effect on the power level.

For telecommunications applications, FM noise is usually measured at 10 KHz off the carrier. The figure obtained was $\Delta_{frms} = 0.42$ Hz/√Hz over a 1-Hz band, which is comparable to those results obtained when the resonator is used as a feedback device [5] or as an output filter [3]. While the goal design was not power efficiency, the measured figure was $\eta_{add} = 14$ percent, showing that the GaAs FET is an inherently efficient device for microwave power generation. Frequency pushing for ±1-V power supply variation was 0.7 MHz, which is also a reasonable figure. A tuning range of at least 50 MHz is possible without degradation of the above mentioned results.

VI. Conclusions

A simple, but accurate, approach for designing stabilized GaAs FET oscillators with a dielectric resonator placed at the input was described. It is sufficient to measure the input reflection coefficient of the active device, at the operational conditions, to determine the position where the dielectric resonator should be placed. A fairly good prevision of the output power is consequently obtained. The advantage of this configuration over the output filter one is that, typically, 3 dB more output power can

be obtained. Over the feedback configuration, the main advantages are the design simplicity and flexibility of output circuitry choice. Noise performance was observed to be comparable to the other two above-mentioned configurations.

ACKNOWLEDGMENT

The authors are indebted to J. C. Mage from Thomson-LCR-Corbeville, for supplying the dielectric resonators.

REFERENCES

[1] P. C. Wade, "Say hello to power FET oscillators," *Microwaves*, pp. 104–109, Apr. 1979.

[2] J. K. Plourde and C. Ren, "Application of dielectric resonators in microwave components," *IEEE Trans. Microwave Theory Tech.*, vol. MTT-29, pp. 754–770, Aug. 1981.

[3] H. Abe, Y. Takayama, A. Higashisaka, and H. Takamizawa, "A highly stabilized low-noise GaAs FET integrated oscillator with a dielectric resonator in the *C*-band," *IEEE Trans. Microwave Theory Tech.*, vol. MTT-26, pp. 156–162, Mar. 1978.

[4] K. Shirata, "Stabilization of solid-state microwave oscillator by loading BFR," in *Proc. Eur. Microwave Conf.*, (London), Sept. 1969.

[5] T. Mori, O. Ishirara, O. Nakatani, and T. Ishi, "A highly stabilized 9–14 GHz FET oscillator using a dielectric resonator feedback circuit," in *IEEE MTT-S Int. Symp. Dig.*, (Washington), May 1980, pp. 376–378.

[6] W. Wagner, "Oscillator design by device line measurement," *Microwave J.*, pp. 43–48, Feb. 1979.

[7] K. Kurokowa, "Some basic characteristics of broad-band negative resistance oscillator circuits," *Bell Syst. Tech. J.*, vol. 48, pp. 1937–1955, July 1969.

[8] K. Johnson, "Large signal GaAs MESFET oscillator design," *IEEE Trans. Microwave Theory Tech.*, vol. MTT-27, pp. 217–227, Mar. 1979.

[9] Y Mitsui, M. Nakatani, and S. Mitsui, "Design of GaAs MESFET oscillator using large signal *S*-parameters", *IEEE Trans. Microwave Theory Tech.*, vol. MTT-25, pp. 981–984, Dec. 1977.

[10] T. Okita, M. Kanazawa, K. Akiba, T. Kogo, and M. Ohno, "Integrated SHF converter simplifies satellite broadcasting," *Microwave Syst. News*, pp. 55–57, June 1979.

[11] Y. Komatsu, Y. Murakami, T. Yamaguchi, T. Otobe, and M. Hirabayashi, "A frequency-stabilized MIC oscillator using a newly developed dielectric resonator," in *IEEE MTT-S Int. Symp Dig.*, (Los Angeles), June 1981, pp. 313–315.

[12] Y. Konishi, N. Hoshino, and Y. Utsumi, "Resonant frequency of a $TE_{01\delta}$ dielectric resonator," *IEEE Trans. Microwave Theory Tech.*, vol. MTT-24, pp. 112–114, Feb. 1976.

[13] A. Podcameni, L. F. M. Conrado, and M. M. Mosso, "Unloaded quality factor measurement for MIC dielectric resonator applications," *Electron. Lett.*, vol. 17, pp. 656–658, Sept. 3, 1981.

[14] C. M. Krowne, "Network analysis of microwave oscillators using microstrip transmission lines," *Electron. Lett.*, vol. 13, pp. 114–117, Feb. 17, 1977.

[15] J. M. Golio and C. M. Krowne, "New approach for FET oscillator design," *Microwave J.*, pp 59–61, Oct. 1978.

[16] J. Obregon, "Contribution à la conception et à la réalization des dispositifs actifis micro-ondes à l'état solide," doctoral thesis, Université de Limoges, pp. 167–218, Mar. 1980.

[17] D. J. Esdale and M. J. Howes, "A reflection coefficient approach to the design of one-port negative impedance oscillators," *IEEE Trans. Microwave Theory Tech.*, vol. MTT-29, pp. 770–776; Aug. 1981.

Coupling Between Microstrip Line and Image Guide Through Small Apertures in the Common Ground Plane

JING-FENG MIAO AND TATSUO ITOH, FELLOW, IEEE

***Abstract*—A design theory is described for coupling between microstrip line and image guide through small coupling holes in a common ground plane. A five-slot Chebyshev coupler is designed based on coupling through a rectangular slot. The theoretical results are compared with experimental results.**

Manuscript received September 2, 1982; revised November 30, 1982. This work was supported in part by U.S. Army Research Contract DAAG 29-81-K0053.

The authors are with the Department of Electrical Engineering, University of Texas at Austin, Austin, TX 78712.

I. INTRODUCTION

During the past several years, much work has been done on the image guide for millimeter-wave circuit applications. Since the image guide is an open structure, any discontinuity created in it causes radiation loss. To minimize radiation in coupling structures, Solbach [1] proposed to locate coupling slots in the ground plane. In the present work, we study the coupling between an image guide and a microstrip line through slots in the common ground plane. This arrangement may be used for sampling the signal in the image guide, or for diverting a part of the power in the image guide into a solid-state device mounted in a microstrip circuit.

We have designed a 15-dB five-slot Chebyshev array coupler based on an approximate theory. The latter is essentially an application of the small-hole analysis found in a standard textbook [2]. This method has also been applied recently to the problem of coupling between two image guides through holes in a common ground plane [3]. Although we neglected radiation completely in the analysis, the measured properties of the directional coupler fabricated in accordance with the present theory have been found to agree well with theoretical predictions.

II. FIELDS IN WAVEGUIDE STRUCTURES

The coupling structure, shown in Fig. 1, consists of an image guide and a microstrip line on opposite sides of a ground plane. The coupling element is either a circular hole or a rectangular slot in the ground plane. The coordinate system is shown in Fig. 1(a) where the z direction is defined as the direction of propagation. Before studying the coupling problem, we obtain simplified expressions of the fields in both the image guide and the microstrip line. Specifically, the expressions developed by Marcatili [4] are used for the image guide, and those for the equivalent parallel-plate waveguide model are used for the microstrip line. Introduction of such "closed-form" expressions considerably simplifies the calculation of the coupling coefficients.

Under Marcatili's model, the transverse fields of the E_{11}^{y} mode are readily given. Here we present only those in the dielectric region ($|x| < a$, $-b < y < 0$ in Fig. 1(b))

$$\bar{E}_{yd}^{\pm} = \hat{y} E_0 \cos(k_x x) \cos(k_y y) \exp(\mp jk_{zd} z) \tag{1a}$$

$$\bar{H}_{xd}^{\pm} = \mp \hat{x} E_0 \frac{1}{\eta} \cos(k_x x) \cos(k_y y) \exp(\mp jk_{zd} z) \tag{1b}$$

$$\eta = \sqrt{\frac{\mu_0}{\epsilon_0}} \frac{k_0}{k_{zd}}$$

where superscripts "+" and "−" represent the propagation along the positive and negative z directions, respectively. $\hat{x}$ and $\hat{y}$ are the unit vectors in the x and y directions. k_x, k_y, and k_{zd} are the propagation constants in the x, y, and z directions, respectively. k_0 is the propagation constant in the free-space. ϵ_0 and μ_0 are the permittivity and permeability in free-space.

The equivalent waveguide model of the microstrip line is shown in Fig. 2. The effective width W' and the effective dielectric constant $\epsilon_{r\text{eff}}$ are such that the TEM mode in the equivalent structure has the same characteristic impedance and phase velocity as the microstrip line. We make use of the expressions derived

0018-9480/83/0400-0361$01.00 ©1983 IEEE